

To describe the **degassing reactions**, the element removal rates in vacuum vessel and ladle have to be calculated separately. The exchange of degassed steel between vacuum vessel (weight W_V , element content X_V with $X = C, H, N$) and ladle (weight W_L , element content X_L) with the steel circulation rate Q_M results in the ladle degassing rate

$$-\frac{dX_L}{dt} = \frac{Q_M}{W_L} \cdot (X_L - X_V) \quad (1)$$

In addition to this steel exchange, for the vessel the degassing reaction under vacuum is described by a first order differential equation of a diffusion process in liquid steel, Kleimt et al (1):

$$-\frac{dX_V}{dt} = -\frac{Q_M}{W_V} \cdot (X_L - X_V) + \frac{1}{T_{XV}} \cdot (X_V - X_Q) \quad (2)$$

The reaction time constant T_{XV} is a model parameter which summarises the mass transport coefficient of the corresponding element and the reaction surface in relation to the steel weight. X_Q is the respective equilibrium content in the gas bubbles near below the bath surface, see Kleimt et al (2). Combining these equations gives the degassing rate of the total heat (2):

$$-\frac{dX}{dt} = \frac{1}{T_X} \cdot (X - X_Q) \quad (3)$$

with the effective time constant

$$T_X = \frac{W}{W_V} \cdot T_{XV} + \frac{W_L}{Q_M} \quad (4)$$

The steel amount in the vacuum vessel is given by the pressure difference between vessel and atmosphere and the vessel geometry. The **steel circulation rate** is calculated depending on vessel pressure and lift gas flow rate according to a mathematical model of Ahrenhold et al (3).

In addition to the mass transfer in the liquid phase, for denitrogenation also the reaction at the liquid / gas interface has to be taken into account, Harada et al (4). This means that in equ. (2) and (3) the equilibrium content N_Q has to be substituted by the interfacial content N_i . The reaction at the liquid / gas interface under vacuum is described by

$$-\frac{dN_V}{dt} = -\frac{Q_M}{W_V} \cdot (N_L - N_V) + \frac{k_{N2}}{k_N \cdot T_{NV}} \cdot (N_i^2 - N_Q^2) \quad (5)$$

with the second order reaction coefficient k_{N2} , divided by the mass transfer coefficient k_N . For the total denitrogenation rate the corresponding additional equation is

$$-\frac{dN}{dt} = \frac{W_V \cdot k_{N2}}{W \cdot k_N \cdot T_{NV}} \cdot (N_i^2 - N_Q^2) \quad (6)$$

The ratio of both kinetic coefficients depends on the contents of the surface-active elements oxygen and sulphur. Values for their influence factors A_O and A_S are given in Bannenberg et al (5), whereas R_N is introduced as a model parameter, Köhle et al (6):

$$\frac{k_N}{k_{N2}} = R_N \cdot (1 + A_O \cdot O + A_S \cdot S) \quad (7)$$

The equations for calculation of the **equilibrium conditions** for the degassing reactions are compiled in **Table I**. The equilibrium content X_Q depends on the partial pressure P_R of the reaction gas ($R = CO, H_2, N_2$) according to equ. (9). The conversion factor F_R used in this equation can be derived from equ. (8) for the equilibrium constant K_X . Using standard values at 1600 °C for K_X , the conversion factor F_R is calculated according to equ. (10). The activity coefficient f_X can be set to 1 for low alloyed steels.

Table I: Equilibrium conditions of degassing reactions

	Decarburisation	Dehydrogenation	Denitrogenation
Equilibrium constant (8)	$K_C = \frac{P_{CO}}{f_C \cdot C_Q \cdot f_O \cdot O_Q}$	$K_H = \frac{\sqrt{P_{H_2}}}{f_H \cdot H_Q}$	$K_N = \frac{\sqrt{P_{N_2}}}{f_N \cdot N_Q}$
Equilibrium content (9)	$C_Q = F_{CO} \cdot P_{CO}$	$H_Q = F_{H_2} \cdot \sqrt{P_{H_2}}$	$N_Q = F_{N_2} \cdot \sqrt{P_{N_2}}$
Conversion equilibrium content (10)	$F_{CO} = \frac{0.002}{f_C \cdot f_O \cdot O_Q} \cdot \frac{\%^2}{\text{bar}}$	$F_{H_2} = \frac{0.0025}{f_H} \cdot \frac{\%}{\text{bar}^{1/2}}$	$F_{N_2} = \frac{0.0434}{f_N} \cdot \frac{\%}{\text{bar}^{1/2}}$
Conversion gas flow rate (11)	$F_{DC} = \frac{22.4 \text{ m}^3}{12 \text{ kg}} \cdot \frac{W}{100\%}$	$F_{DH} = \frac{22.4 \text{ m}^3}{2 \text{ kg}} \cdot \frac{W}{100\%}$	$F_{DN} = \frac{22.4 \text{ m}^3}{28 \text{ kg}} \cdot \frac{W}{100\%}$

The partial pressure of the reaction gas near below the bath surface results from the vacuum vessel pressure P_{GV} , an additional pressure P_{ZV} , and the concentration of the reaction gas which is diluted by the process gas with the flow rate Q_D :

$$P_R = (P_{GV} + P_{ZV}) \cdot \frac{F_{DX} \cdot D_X}{F_{DX} \cdot D_X + R_{VQ} \cdot Q_D} = (P_{GV} + P_{ZV}) \cdot R_Q \quad (12)$$

The reaction gas flow rate is proportional to the degassing rate, abbreviated as D_X , with the factor F_{DX} from equ. (11). The process gas consists of the lift gas with the flow rate Q_P and the gases of the degassing reactions which occur besides the reaction for the element X. R_Q is the resulting dilution ratio. With the model parameter R_{VQ} it is considered that the dilution of the reaction gas mainly occurs in the part of steel which is above the up-leg snorkel of the vacuum vessel, which reduces the dilution effect.

With the additional pressure P_{ZV} it is taken into account that the expansion of the ascending gas bubbles is impeded because they have to accelerate the surrounding steel, see Szekely et al (7). From theoretical investigations in Köhle et al (6) it was found, that the additional pressure near below the bath surface depends on the vessel pressure according to

$$P_{ZV} = P_{ZE} \cdot \exp[-P_{GV} / (2 \cdot P_{ZE})] \quad (13)$$

The additional pressure P_{ZE} for $P_{GV} = 0$ is a model parameter, which has to be identified from the degassing behaviour. Its value is with about 40 mbar much higher than the vessel pressure itself.

The steel **oxygen removal** rate can be calculated from the decarburisation rate to:

$$-\frac{dO}{dt} = \frac{16}{12} \cdot R_{CO} \cdot \left(-\frac{dC}{dt}\right) \quad (14)$$

With the steel oxygen removal ratio R_{CO} it is considered that a part of oxygen is not provided from the steel but by reduction of oxides in the ladle slag. Adverse than expected, R_{CO} increases with higher slag oxide concentrations, as they are combined with higher oxygen and lower carbon contents in the steel bath due to the preceding treatment in the LD converter. The reason is that the oxygen

solved in the steel can easier be supplied for the decarburisation reaction than the one coming from slag oxides. Therefore the steel oxygen removal ratio can be estimated from the

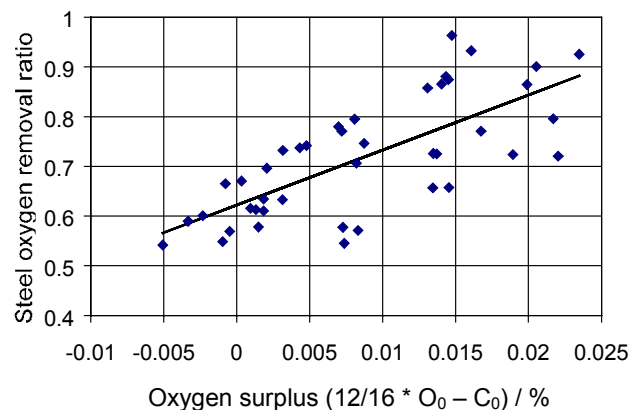


Fig. 2: Steel oxygen removal ratio versus oxygen surplus

oxygen and carbon contents O_0 and C_0 analysed before vacuum treatment, as shown in **Fig. 2**.

The **temperature decrease** during vacuum treatment is calculated as:

$$-\frac{dT}{dt} = RT_L + RT_V \cdot \exp(-t/T_{RTV}) \quad (15)$$

With the constant temperature loss rate RT_L the radiation losses in the ladle are taken into account. An additional dynamic temperature loss due to heat transfer of the circulating steel to the vessel lining is described by an exponential function. Starting from an initial loss rate RT_V , which mainly depends on the thermal state of the vacuum vessel, the loss rate decreases with the time constant T_{RTV} to almost zero at the end of vacuum treatment, due to the diminished intensity of the degassing reactions and the approach of a steady-state thermal condition of the vacuum vessel. The influence of material additions is considered by the material-specific chilling factor given in $K / (kg / t)$, that means the temperature decrease after addition of one kg to one ton of liquid steel. The temperature increase by deoxidation with aluminium after decarburisation is calculated from the corresponding oxygen removal based on thermodynamic relations.

MODEL VERIFICATION AND SIMULATION RESULTS

The process model was installed on a PC for dynamic simulation under MATLAB and SIMULINK. It was verified by comparison of simulation results with measured process data from the RH/1 plant of VASL. The degassing behaviour and the evolution of steel temperature were simulated based on the heat-specific start values which are the analysed contents of carbon and nitrogen as well as Celox respectively Hydrys measurements for steel temperature, oxygen and hydrogen content. Input values for the simulation are the cyclically measured values for vessel pressure and lift gas flow rate, as well as type and amount of material additions during vacuum treatment. The model parameters were optimised for each heat by minimising the deviations between the simulation results and the corresponding analysed respectively measured values during and after vacuum treatment. For verification of the decarburisation behaviour, additionally cyclically measured values for waste gas flow rate and CO / CO_2 content were used. In the following simulation results for different example heats which are based on the adapted model parameters are shown, together with the model accuracy which was achieved with parameter mean values resulting from the optimisation results of all evaluated heats. The simulation error for the different degassing reactions and the steel temperature is given in **Table II**.

For verification of the **decarburisation** model, the data of 40 unkilld heats were evaluated. **Fig. 3** shows the simulated decarburisation rate in comparison to the one calculated from the measured waste gas values. Additionally the simulated carbon content is displayed together with the analysed final value, and the oxygen content with the measured one before deoxidation. In **Fig. 4 and 5** the analysed respectively measured final carbon and oxygen contents are compared to the simulation results based on mean parameter values for all heats.

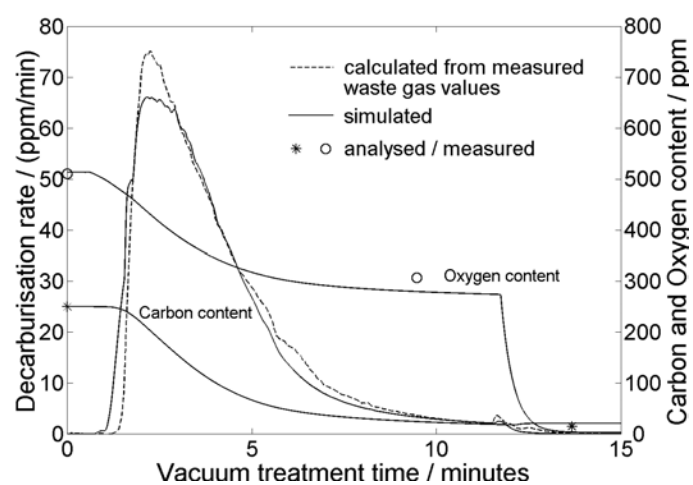


Fig. 3: Decarburisation simulation

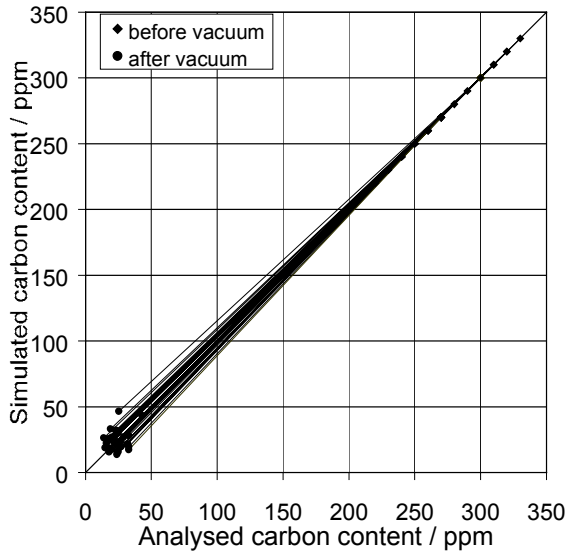


Fig. 4: Simulated versus analysed carbon content during RH treatment

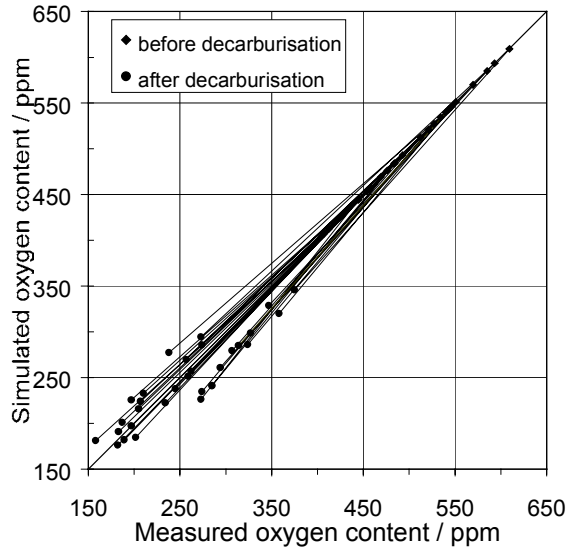


Fig. 5: Simulated versus measured oxygen content during RH treatment

Verification of the **dehydrogenation** model was performed with the data of 30 deoxidised heats. **Fig. 6** shows for two example heats the simulation results with optimised parameters, together with Hydrys measurements. The good simulation accuracy is also proven with **Fig. 7**, where the simulation results of the final hydrogen content based on mean parameter values are shown for all heats.

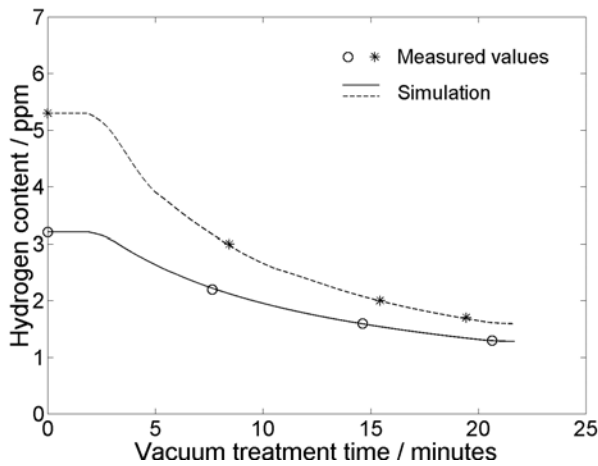


Fig. 6: Dehydrogenation simulation

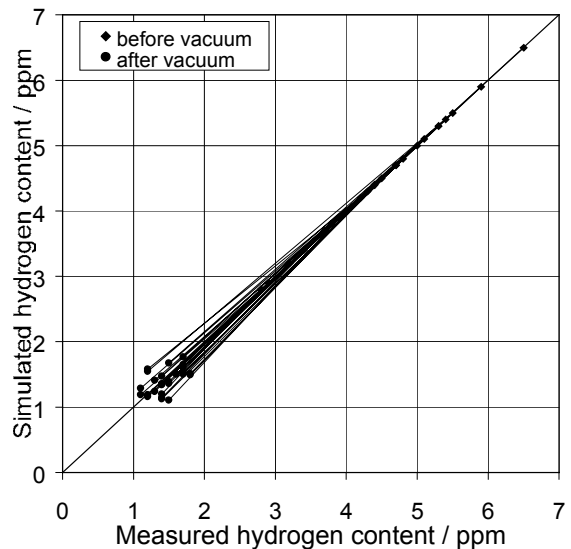


Fig. 7: Simulated versus measured hydrogen content during RH treatment

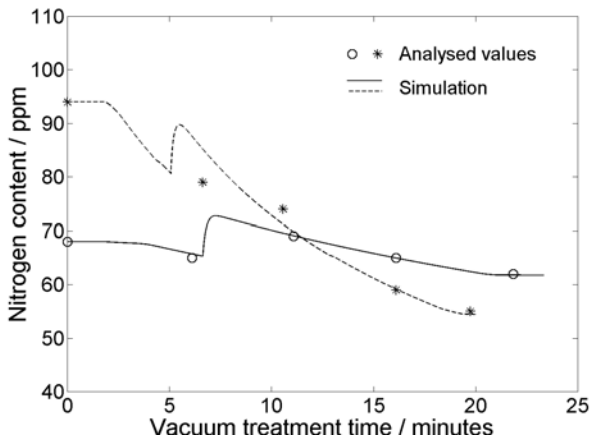


Fig. 8: Denitrogenation simulation

The accuracy of the **steel temperature** simu-

lation was checked for all evaluated heats. For verification of the **denitrogenation** model the nitrogen pickup from material additions had to be taken into account. Due to the uniform sulphur content of the 46 evaluated heats with 30 ppm on the average, no significant influence on denitrogenation occurred. **Fig. 8** shows the nitrogen simulation based on optimised model parameters for two heats, together with the analysed nitrogen content. In **Fig. 9** the simulation results of all evaluated heats are displayed.

Fig. 10 shows the simulation results for two deoxidised example heats, which were the first and the last heat of a sequence of in total four heats. For the first heat, the dynamic vessel temperature loss rate is much higher than for the last one. This effect of the thermal vessel state can clearly be seen in the temperature drop during the first 5 minutes of treatment. After about 10 minutes, thermal steady-state conditions are reached. As for most of the evaluated heats no information on the thermal state of the vacuum vessel was available, its influence on the parameters for the vessel temperature loss rate could not be considered, and mean values had to be used. **Fig. 11** shows as an example a comparison between the measured and the simulated temperature during vacuum treatment for 29 deoxidised heats.

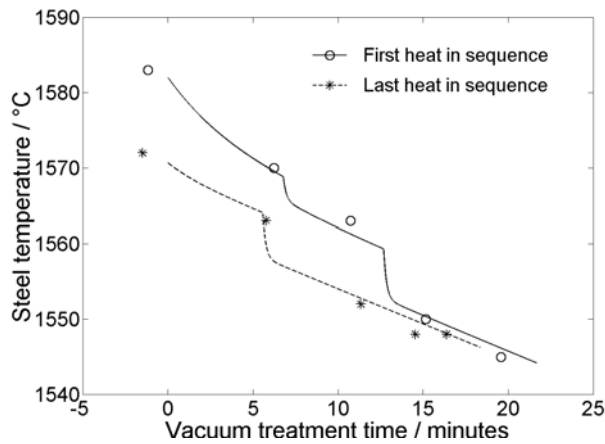


Fig. 10: Temperature simulation for two heats of a sequence

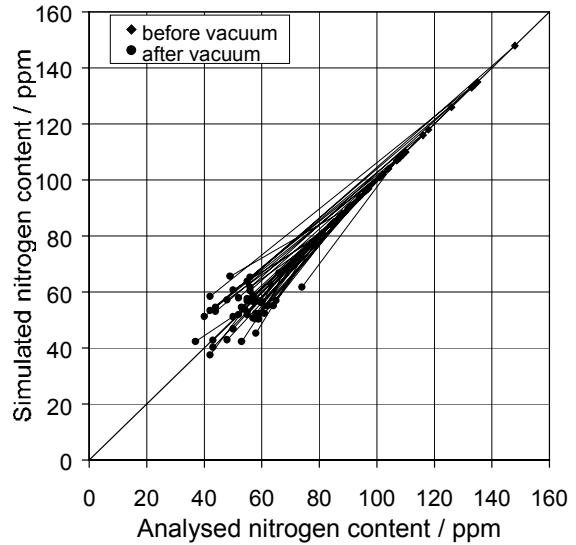


Fig. 9: Simulated versus analysed nitrogen content during RH treatment

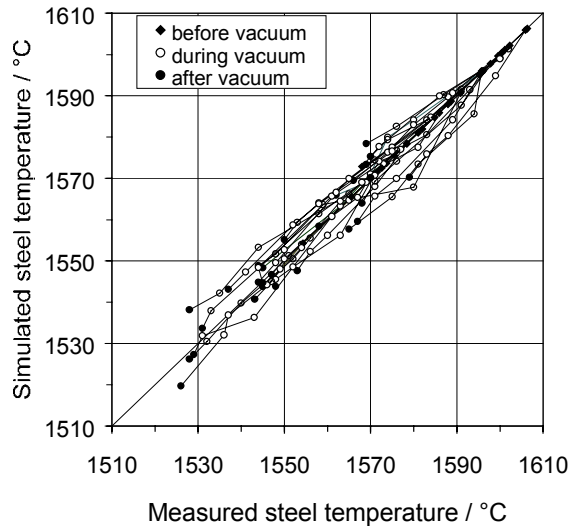


Fig. 11: Simulated versus measured temperature during RH treatment

Table II: Accuracy of the process model concerning the different degassing reactions and the steel temperature

Degassing reaction	Number of heats	Simulation error / ppm	
		Mean value	Standard deviation
Decarburisation / Final carbon content	40	2.4	8.7
Decarburisation / Carbon content before deox.	40	-2.3	7.8
Decarburisation / Oxygen content before deox.	40	-6.0	22.8
Dehydrogenation / Final hydrogen content	30	0.002	0.2
Denitrogenation / Final nitrogen content	46	-0.02	7.6
Steel temperature / During RH treatment	116	0.4 K	5.4 K

APPLICATION OF THE PROCESS MODEL FOR ON-LINE OBSERVATION

The model was applied for process observation, that means the continuous calculation of the carbon, oxygen, nitrogen and hydrogen content of steel as well as the steel temperature during vacuum treatment. To simplify the process model for this on-line application, the element concentrations $X = C, H, N$ of steel in the vacuum vessel and in the ladle are not calculated separately, but as common concentrations of the total heat. The resulting total degassing rate is given in equ. (3) with the effective time constant T_X of equ. (4). The steel amounts W_V and W_L as well as the steel circulation rate Q_M , which are required to calculate this effective time constant, change during vacuum treatment. As the vessel pressure decreases, the steel amount in the vacuum vessel increases, and the steel circulation starts with also increasing rate. But as after approximately 3 minutes steady-state values for W_V and Q_M are reached, a constant mean value for the effective time constant can be chosen for each degassing reaction. The accuracy of the process model is only slightly decreased by this simplification.

The required input values for the model-based on-line observation system are:

- cyclically measured vessel pressure and lift gas flow rate
- analysed contents of carbon, sulphur and nitrogen before start of vacuum
- measured start values of oxygen content and steel temperature
- start steel weight
- material additions during vacuum treatment

The measured or analysed hydrogen content at treatment start is not required as it has only a small influence on the finally achieved content, see Köhle et al (6).

To improve the accuracy of the decarburisation observation, the cyclically measured values of waste gas flow rate Q_A and its CO / CO_2 content can be used. From these values the current decarburisation rate can be calculated to:

$$-\frac{dC}{dt} = (K_{CO} + K_{CO_2}) \cdot Q_A \cdot \frac{1}{F_{DC}} = \frac{Q_{CO}}{F_{DC}} \quad (16)$$

With the analysed start content C_0 as initial value, integration of the decarburisation rate gives the current carbon content of the heat. Systematic errors in this carbon balance due to the measured waste gas values can be partially compensated by a correction factor, which is adapted after each heat so that the final content from the carbon balance is equalised to the analysed one. A moving average of this correction factor over a number of preceding heats can be used for the next heat. However, by this method irregular errors of the waste gas measurement and errors in steel weight and start carbon content cannot be corrected. An evaluation of the carbon balance based on waste gas values revealed that the accuracy of the observed final carbon content is with an error mean value of 7 ppm and a standard deviation of 26 ppm very poor.

To improve the accuracy of the carbon balance, a model-based on-line correction calculation was developed, which uses the almost linear relation between decarburisation rate and carbon content during the final phase of decarburisation. As described in detail in Kleimt (2), this relation can be derived from equ. (3), (9) and (12) and can be expressed as:

$$-\frac{dC}{dt} \cdot T_C = C - C_E \cdot R_Q \quad (17)$$

C_E is the carbon content, which would finally be reached without the dilution effect by the process gas ($R_Q = 1$). It is in equilibrium with the final oxygen content at the final bubble pressure, which is mainly determined by the additional pressure P_{ZV} . Due to the dilution ratio R_Q , this equation is non-linear and can be linearised by introduction of a modified carbon content C_{RQ} :

$$-\frac{dC}{dt} \cdot T_C = C + (1 - R_Q) \cdot C_E - C_E = C_{RQ} - C_E \quad (18)$$

C_{RQ} can be calculated on-line, using the cyclically measured process gas flow rate, and the CO flow rate as well as the carbon content resulting from waste gas values as described in equ. (16):

$$C_{RQ} = C + \left(\frac{R_{VQ} \cdot Q_D}{Q_{CO} + R_{VQ} \cdot Q_D} \right) \cdot C_E \quad (19)$$

In **Fig. 12** the decarburisation rate from the carbon balance, using the moving average correction, is plotted versus the resulting carbon content C and versus C_{RQ} for the example heat of Fig. 3. In the final stage of decarburisation the first curve deviates from its linear course due to the CO dilution by the process gas. By introduction of the modified carbon content C_{RQ} , the linear section of the curve is extended almost up to the end of decarburisation. As indicated for the nearly linear part of the curve, a regression line can be calculated and extrapolated to the point when the decarburisation rate becomes zero.

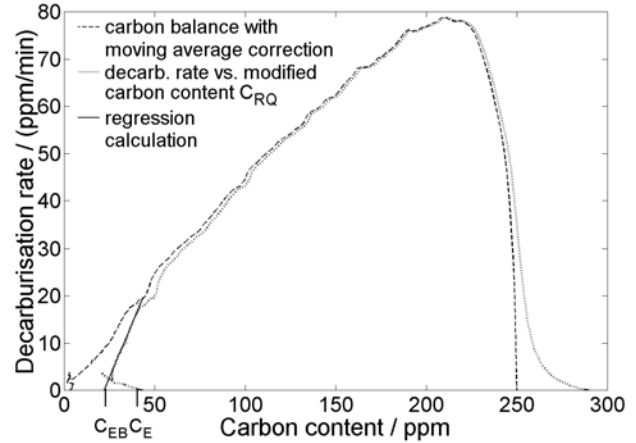
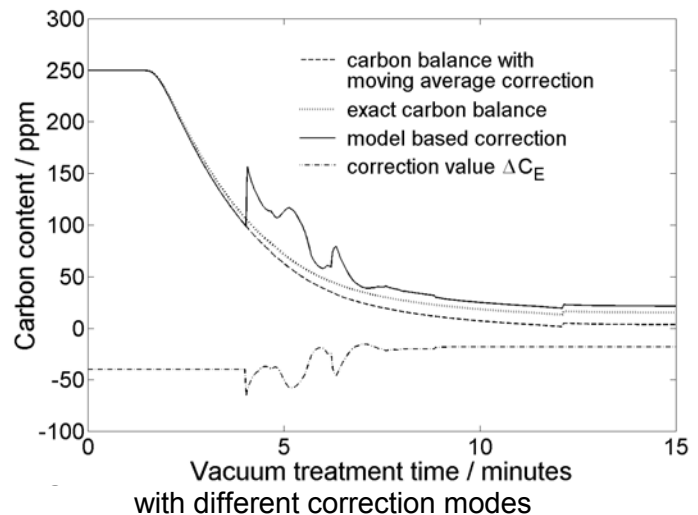


Fig. 12: Decarburisation diagram of model-based correction calculation

As equ. (18) describes, at this point the modified carbon content C_{RQ} should reach on the average a representative mean value of C_E , which is indicated in the figure. For the example heat the extrapolation results in a final carbon content C_{EB} which deviates from the expected one. The difference of these two carbon contents ΔC_E can be used for correction of the carbon content which results from the carbon balance. This correction calculation was applied to the 40 decarburisation heats which were used for model verification, to check if the accuracy of observation concerning the final carbon content can be improved. **Fig. 13** shows the result for the example heat of Fig. 12. As a reference the carbon contents resulting from the balance with correction by the moving average value and with a heat-individual value which leads to the exact final carbon content are plotted. As can be seen the correction value ΔC_E changes during the regression calculation together with the slope of the decarburisation diagram. The regression calculation is stopped after approximately 9 minutes because the correlation coefficient becomes too low. By this it is ensured that only the linear section of the decarburisation diagram is used

for extrapolation. From this point on ΔC_E is fixed up to the end of treatment. The resulting observed final carbon content is the most accurate one with respect to the analysed one. **Fig. 14** shows the accuracy improvement of the carbon balance which was achieved with the model-based correction calculation. The error standard deviation of the final carbon content was reduced from 26 ppm to 6 ppm, which is also an improvement of about 2 ppm compared to the error achieved without using the measured waste gas values, see Table II. A similar correction calculation was developed for the VOD process, see Köhle et al (8).



The on-line observation model was converted into a C programme and installed on a PC at the RH/1 plant of Voest Alpine Stahl Linz. It is currently tested and evaluated concerning its accuracy in daily operation practice. The required input data are transferred from existing process computers via appropriate interfaces. For the new RH/2 plant, the observation model will be implemented directly within the process computer system.

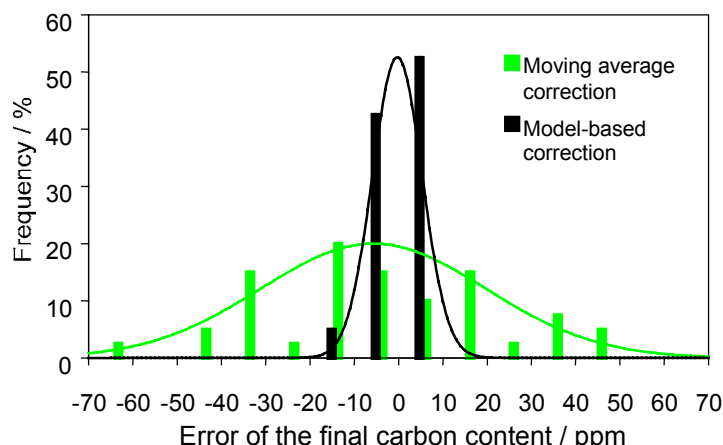


Fig. 14. Accuracy improvement of the carbon balance

CONCLUSIONS AND PROSPECTS

The developed on-line observation system calculates the current heat status during RH treatment with good accuracy and therefore allows to reduce the number of samples as well as temperature and Celox measurements. Furthermore the time can be determined when the required final contents of carbon, hydrogen and nitrogen are achieved. This means that it is not required to elongate the vacuum treatment time more than necessary. At the RH plants of VASL it will be extended to nitrogen pickup by lift gas and the influence of oxygen supply via a top lance. In calculating the steel temperature, the influence of the thermal vessel state will be considered.

ACKNOWLEDGEMENTS

The on-line observation system for the RH process was developed within an ECSC research project. The authors like to thank the ECSC for their financial support.

LIST OF SYMBOLS (including model parameter values for the RH/1 plant of VASL)

Symbol	Meaning	Value	Unit
A_O	factor of oxygen effect on denitrogenation	770	1/%
A_S	factor of sulphur effect on denitrogenation	620	1/%
C_E	final carbon content without CO dilution	0.004	%
C_{EB}	final carbon content from extrapolation of waste gas values		%
C_{RQ}	carbon content without CO dilution effect		%
f_X	activity coefficient of element X (X = C, H, N, O)		1
F_{DX}	conversion factor degassing rate to gas flow rate (X = C, H, N)		m ³ /%
F_{CO}	conversion factor CO partial pressure to C equilibrium		% ² /bar
F_R	conversion factor partial pressure to equilibrium (R = H ₂ , N ₂)		%/bar ^{1/2}
k_N	mass transfer coefficient of N		m/s
k_{N2}	second order reaction coefficient of N		m/s/%
K_{CO}	CO concentration of waste gas		%
K_{CO2}	CO ₂ concentration of waste gas		%
K_X	equilibrium constant of element X (X = C, H, N)		1
O	Oxygen content of steel		%
P_R	partial pressure of reaction gas (R = CO, H ₂ , N ₂)		bar
P_{GV}	vacuum vessel pressure		bar
P_{ZV}	additional pressure due to steel acceleration		bar
P_{ZE}	additional pressure at $P_G = 0$	0.043	bar
Q_A	waste gas flow rate		m ³ /h
Q_{CO}	CO gas flow rate		m ³ /h

Q_D	process gas flow rate		m^3/h
Q_M	steel circulation rate		t/min
Q_P	lift gas flow rate		m^3/h
R_{CO}	steel oxygen removal ratio		1
R_{VQ}	dilution efficiency of process gas	0.65	1
R_N	coefficient of denitrogenation kinetics	0.006	%
R_Q	dilution ratio in a gas bubble		1
R_{TL}	ladle radiation temperature loss rate	0.93	K/min
R_{TV}	start value for vessel temperature loss rate vessel	2.0	K/min
S	sulphur content of steel		%
t	time		s
T	steel temperature		$^{\circ}C$
T_X	effective time constant of degassing ($X = C, H, N$)	70 / 124 / 294	s
T_{XV}	reaction time constant of degassing ($X = C, H, N$)	0.5 / 4.5 / 17.5	s
T_{RTV}	time constant for decrease of vessel temp. loss rate	2.92	min
X	element content of steel ($X = C, H, N$)		%
W	steel weight		t

Indices

L	in the ladle	V	in the vacuum vessel		
Q	at equilibrium	i	at liquid / gas interface	0	at treatment start

REFERENCES

- (1) Kleimt B, Köhle S, 'Dynamic modelling of vacuum circulation process for steel decarburization', La Revue de Métallurgie - CIT, Avril 1995, p. 493 - 502
- (2) Kleimt B, Köhle S, Johann K, Jungreithmeier A, Molinero J, 'Dynamic process model for denitrogenation and dehydrogenation by vacuum degassing', SCANMET I, Lulea 1999, Vol. 2, p. 241-265, and Scandinavian Journal of Metallurgy, Vol. 29, No. 5, p. 194-205.
- (3) Ahrenhold F, Pluschkell W, 'A New Mathematical Model of the Circulation Flow in RH Units', Scaninject VII, Lulea 1995, p. 83 - 106.
- (4) Harada T, Janke D, 'Nitrogen desorption from pure iron melts under reduced pressure', Steel research 60 (1989), No. 8, p. 337 - 342
- (5) Bannenberg N, Bergmann B, Gaye H, 'Combined decrease of sulphur, nitrogen, hydrogen and total oxygen in only one secondary steelmaking operation', Steel research 63 (1992), No. 10, p. 431 - 437
- (6) Köhle S, Kleimt B, Lichterbeck, R, 'Dynamic modelling and control of the vacuum degassing process', BFI report 2.32.004, Stahl-Zentrum Düsseldorf, 2000
- (7) Szekely J, Martins G. P, 'Studies in Vacuum Degassing. Part I: Fluid Mechanics of Bubble Growth at Reduced Pressure', Transactions of the Metallurgical Society of AIME 245 (1969), p. 629 - 636
- (8) Köhle, S, Reichel J, Heinen K, Dittert D, 'Dynamic modelling and control of the VOD process', 5th International Iron and Steel Congress, Washington 1986, p. 257-265